Carbohydrate Polymers 82 (2010) 1219–1227

Contents lists available at ScienceDirect

Carbohydrate Polymers

journal homepage: www.elsevier.com/locate/carbpol

Weak-gel formation in dispersions of silica particles in a matrix of a non-ionic polysaccharide: Structure and rheological characterization

Fabiane Oliveira [a], Sónia R. Monteiro [b], Ana Barros-Timmons [a], J.A. Lopes-da-Silva [b,*]

[a] CICECO – Centre for Research in Ceramics and Composite Materials, Departamento de Química, Universidade de Aveiro, 3810-193 Aveiro, Portugal
[b] QOPNA – Organic Chemistry, Natural and Agrofood Products Research Unit, Departamento de Química, Universidade de Aveiro, 3810-193 Aveiro, Portugal

ARTICLE INFO

Article history:
Received 4 April 2010
Received in revised form 3 June 2010
Accepted 28 June 2010
Available online 31 July 2010

Keywords:
Polysaccharide/inorganic composites
Locust bean gum
Silica particles
Rheology
Cryo-SEM
Gelation

ABSTRACT

Oscillatory and steady-shear rheological methods as well as scanning electron microscopy were used to characterize silica (SiO_2)/galactomannan dispersions. Particle loading and surface charge are found to strongly influence the composite structure and dynamics. When the particles were added above a minimum concentration, a sol–gel transition was induced. The SiO_2/polysaccharide dispersions exhibited significant non-linearities, especially under ionic conditions that favor interparticle and particle–polysaccharide interactions, characterized by strong shear-thinning, diverging viscosities at low shear rates, apparent yield stress and high strain sensitivity. The mechanical spectra for the composite systems suggest that stress relaxation of these composites is effectively arrested by the presence of silica nanoparticles. Microstructural analysis revealed an ordering of the silica particles around the polymer chains. Polysaccharide chains act as templates for particle clustering leading to the formation of a particle-mediated transient biopolymer network, with particle clusters hindering polymer mobility and enhancing junction zones within the network.

1. Introduction

The preparation of inorganic/biopolymer nanocomposites is an attractive strategy for the development of novel materials with interesting and tailorable properties. These composites combine the advantages of both the inorganic material and the organic polymer, often providing improved properties to the composite. One important feature is the remarkable increase in the interfacial area, due to the small size of the fillers, creating a significant volume fraction of interfacial polymer with properties different from the bulk polymer even at low loadings.

Many studies on the linear viscoelastic properties of polymer nanocomposites, mainly for filled polymer melts with a diversity of fillers (clays, carbon nanotubes, silica particles, etc.), have suggested that strong enhancements in the elasticity of these systems occur with increasing concentrations of the filler, often manifested by transitions from liquid-like to solid-like rheological behaviour at relatively low particle loadings, and solid-like behaviour with a plateau in the storage modulus $G'(\omega)$ persisting at even very low frequencies (Du et al., 2004; Krishnamoorti & Yurekli, 2001; Metzner, 1985; Paquien, Galy, Gerard, & Pouchelon, 2005; Solomon, Almusallam, Seefeldt, Somwangthanaroj, & Varadan, 2001; Zhang & Archer, 2002). At high nanoparticle concentrations, physical gelation, elasticity and the formation of composite networks are strongly dependent on the polymer-filler interactions. For high concentrations of non-adsorbing polymers, depletion flocculation is likely to occur pushing the particles into a small volume of concentrated phase, as observed, for example, for polystyrene latex particles in the presence of non-adsorbing sodium carboxymethylcellulose (Trompette & Bordes, 2000). Another possible mechanism responsible for polymer/filler gelation occurs for adsorbing polymers, which can bridge particles together, when the adsorbed layers on the particle surface are unsaturated, forcing the particles to share the available polymer chains, as observed, for example, for such diverse systems as talc particles in cross-linked polyacrylylglycinamide hydrogels (Trompette, Charnay, & Partyka, 1998), or xanthan/silica dispersions (Oh, So, & Yang, 1999).

Among the numerous inorganic/organic nanocomposites, polymer/silica composites are the most commonly reported in the literature (Zou, Wu, & Shen, 2008), and the majority of the examples reported have been prepared using synthetic polymers. However, the use of biopolymers can bring additional advantages to the nanocomposites, related to their renewable sources, biocompatibility and biodegradability, although some of the traditional advantages of the organic polymer (e.g., mechanical resistance, ductility, and processability) may be compromised.

In fact, in recent years, a wide variety of biopolymers have been employed to produce biopolymer/silica nanocomposites and their potential applications investigated (Coradin, Allouche, Boissiere,

* Corresponding author. Tel.: +351 234370360; fax: +351 234370084.
E-mail address: jals@ua.pt (J.A. Lopes-da-Silva).

0144-8617/$ – see front matter © 2010 Elsevier Ltd. All rights reserved.
doi:10.1016/j.carbpol.2010.06.046

& Livage, 2006; Shchipunov & Karpenko, 2004). The reported properties observed for polysaccharide/silica composites are also diverse and strongly dependent on the polymer–particle affinity and interactions. Pashkovski, Masters, and Mehreteab (2003), using mixtures of silica and xanthan gum or carboxymethyl cellulose, described the structure and formation of particulate silica networks and showed that the elasticity of the polymer matrix plays an important role in particle aggregation, including the fractal dimension of the silica network, as well as on the kinetics of structural recovery after preshear.

Shchipunov and co-workers (Shchipunov & Karpenko, 2004; Shchipunov, Karpenko, Krekoten, & Postnova, 2005) have shown that polysaccharides can mediate the formation of hybrid silica nanocomposites by sol–gel processes and that non-gelling polysaccharides, such as chitosan and hyaluronate, can be gelled by generating silica *in situ* via a sol–gel process, using a water-soluble precursor compatible with the biopolymers. In this case gelation was explained by a process resembling biomineralization, causing the polysaccharide chains to strength and to cross-link. Coradin, Bah, and Livage (2004) have studied aqueous solutions of gelatine and sodium silicate under conditions also leading to the formation of silica nanoparticles *in situ*, and found that addition of silica decreases the stability of the gels by inducing gelatine depletion in solution. In this case, the strong interactions between silicates and gelatine lead to composite gels with lower stability than the pure biopolymer gel. In fact, most of the studies on polysaccharide/silica composites have employed a sol–gel method to prepare the silica particles *in situ* from a percursor. We have recently shown (Daniel-da-Silva et al., 2008) that the addition of preformed silica nanoparticles also impairs the gelation of κ-carrageenan, an effect dependent on silica load and particle size and attributed to a steric barrier effect caused by the presence of the silica particles weakening polysaccharide aggregation and gelation, under ionic conditions where both components bear negative charges.

In this work, aiming to investigate the possible development of new thickening and/or soft-gel systems through the formation of biopolymer/inorganic nanocomposites, we have studied the rheology and structure of silica (SiO_2)/polysaccharide dispersions, using dynamic and steady-shear rheological tests and scanning electron microscopy analysis. The biopolymer used was locust bean gum, a random-coil non-ionic galactomannan polysaccharide. The polymer nanocomposites were prepared via a simple blending method of both components, providing uniform dispersion of the silica particles in the biopolymer solution. We foresee that the rheological properties of these dispersions can be tailored by controlling the particle loading and charge, which can be dependent, among other factors, on the pH medium and the composition of the dispersion. Therefore, this study is expected to provide a better understanding on the influence of particle loading and ionic effects on the structure and gelation behaviour of these systems, with practical relevance as models for specific technological applications (e.g., colloidal stability in several industrial processes, adhesives, coatings, etc.).

2. Experimental

2.1. Materials

Tetra-ethyl ortosilicate 98% and hydrochloric acid (Sigma–Aldrich), ammonia aqueous solution 25% (Merck), sodium chloride and acetic acid (Acros), and ethanol (Fluka) were purchased and used as acquired. Locust bean gum (LBG) was purchased from Sigma–Aldrich.

Silica particles were prepared by the Stöber method with some modifications (Pinto, Marques, Barros-Timmons, Trindade, & Neto, 2008) and used after calcination at 700 °C for 4 h. Zeta potential and hydrodynamic particle size measurements were performed using a ZetaSizer Nanoseries instrument from Malvern Instruments. The SiO_2 nanoparticles were essentially spherical with an average diameter of 258 ± 21 nm, a specific surface area of $11 \pm 2\ m^2/g$, and a zeta potential around 0 and −20 mV at pH 3 and 5, respectively (pH values used to prepare the composite dispersions).

2.2. Sample preparation

Silica dispersions (up to 40 wt.%) were prepared by adding the silica powder to water or 0.1 mol/dm^3 NaCl at room temperature, stirring overnight, and then treated by sonication during 1 h. LBG solutions (1.0 wt.%) were prepared in distilled water or in 0.1 mol/dm^3 NaCl by stirring moderately during 1 h at room temperature followed by 30 min at 90 °C. Finally the suspensions were centrifuged at 12,000 rpm for 20 min.

SiO_2/LBG suspensions were prepared by simple mixture of components. Typically LBG solutions and suspensions of SiO_2 particles previously prepared were mixed (1:1), resulting in a final aqueous suspension of 0.5 wt.% LBG and 5, 10 or 20 wt.% of SiO_2 particles. The pH was adjusted with HCl and/or NH_4OH. Finally the dispersion was stirred for 60 min under vacuum, in order to remove air bubbles, before being analysed.

2.3. Rheological measurements

The sample was transferred to the rheometer measuring system right after preparation. All measurements were made at constant temperature (20.0 °C) using a Bohlin CVO HR120 controlled-stress rheometer equipped with a cone-and-plate geometry (4°, 40 mm diameter, 150 μm truncation). The temperature was controlled by a Peltier system built-in the lower fixed flat plate. A solvent trap was used which sealed the sample against the environment using silicone and a low-viscosity mineral oil, in order to keep solvent evaporation from the sample to a minimum throughout the duration of each test.

Time sweep tests, maintaining a small peak strain amplitude, at a fixed frequency ($2\pi\nu = \omega$) of 1 rad/s, were used to ensure that slow relaxation processes were allowed to occur after loading the sample, avoiding any effects of shear during sample loading, and to assess any structure development processes depending on time. The response of the dispersions to changes on strain amplitude was analysed by stress sweep tests at constant frequency (1 rad/s), in order to define the linear viscoelastic region and to select the appropriate strain amplitude (γ_o) to collect the subsequent data or to correct the strain value used in the initial time sweep experiments. The viscoelastic behaviour of the dispersions, namely the frequency dependence of the viscoelastic moduli G' and G'', after certain curing times on the rheometer, was assessed from frequency sweep experiments (0.01–10 rad/s), at low strain amplitude within the linear viscoelastic regime.

Flow curves were obtained by an up–down step program applying a different shear stress range to each sample. The sample was held at each programmed stress for typically 60 s.

2.4. Cryo-scanning electron microscopy (cryo-SEM)

Microstructure of the LBG/SiO_2 composites has been analysed by cryo-scanning electron microscopy (cryo-SEM). Samples were maintained under quiescent conditions during 2 h and frozen under liquid nitrogen. The frozen samples were sublimated at −95 °C during 1 min and the fracture surfaces were coated with Au/Pd during 15 s. Analysis was performed at −140 °C using a FE-SEM JEOL JSM6301F microscope operating at 15 kV and coupled with a cryo-SEM unit Gatan model ALTO 2500.

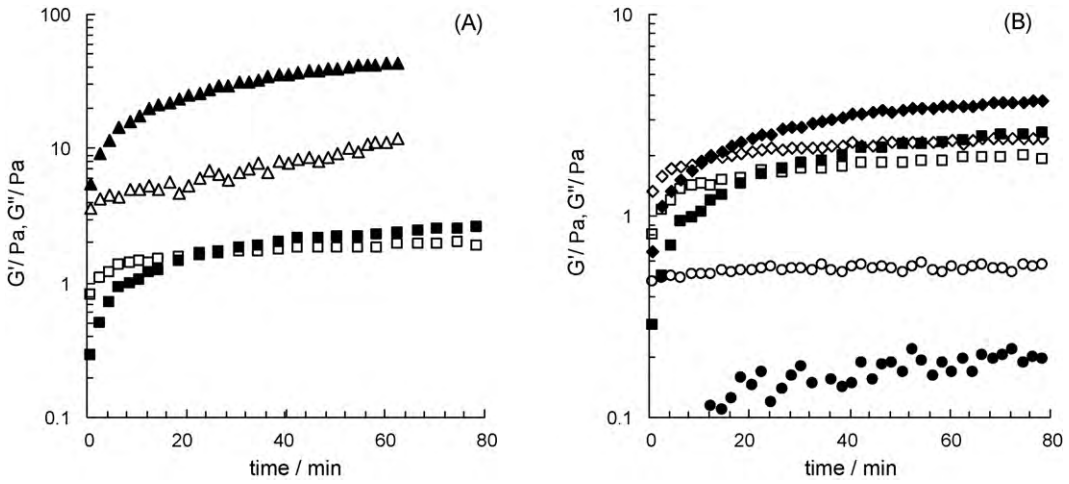

Fig. 1. Evolution of the storage (G', solid symbols) and loss (G'', open symbols) shear modulus with time at $\omega = 1$ rad/s and 20 °C for silica suspensions in 0.5% (w/w) LBG: (A) in water at pH 3 (■, □) and 20 (▲, △) wt.% silica; (B) 10 wt.% silica under different ionic conditions – in water at pH 3 (■, □) and pH 5 (●, ○), and in 0.1 mol/dm^3 NaCl at pH 3 (♦, ◊).

3. Results

3.1. Rheological changes with time at constant frequency

The measured viscoelastic moduli for the LBG solutions alone did not change with time. However, kinetic effects were clearly evident for the LBG/SiO_2 dispersions, especially for particle loadings above 10 wt.%. The recovery time or the aging processes were different for each sample, with a clear dependence on particle concentration and ionic conditions.

Fig. 1 illustrates these effects for 10 and 20 wt.% silica dispersions in 0.5 wt.% LBG solutions, under different ionic conditions. Typical behaviour involved an early stage, a relatively short period, in which the modulus rose more rapidly, then followed by a second, longer period in which the modulus continued to increase at a lower rate. For 5 wt.% silica loadings, little aging effects were observed with small changes on both viscoelastic moduli even after long time periods (24 h).

Both the storage (G') and loss (G'') moduli increased with the aging time. Certain samples showed already at the beginning a high structure with $G' > G''$, as is the case of the 20 wt.% silica/LBG suspensions at pH 3 (Fig. 1A). For the 10 wt.% silica suspensions, initially $G'' > G'$ up to the crossover point, i.e., the point at which G' becomes larger than G'', indicative of a liquid-like to a solid-like transition. At an ionic strength of 0.1 mol/dm^3 the onset of this critical transition occurs faster (Fig. 1B), and an opposite effect was observed by increasing the pH. Therefore, the viscoelastic moduli reach higher values, which correspond to more rigid structures at rest, and the rate of gelation increases as the particle loading increases or the particles charge density decreases (higher ionic strength or lower pH), at least within the ranges analysed for these variables.

3.2. Strain dependence of the viscoelastic response

After aging until the moduli had become stationary, stress sweep tests were performed to characterize the strain dependence of the viscoelastic response for the silica/polysaccharide systems.

The LBG solutions showed a low sensitivity to the applied strain, with linear viscoelastic limits extending to strain values around 100% or even higher (results not shown). However, due to the lower limit of the instrument regarding the displacement measurements, well resolved displacement readings could be obtained only for strain values above 10% or higher.

The strain dependence of the viscoelastic response was noticeably different for the LBG/silica composite dispersions. Fig. 2 shows the typical behaviour of the apparent complex modulus (G^*_{ap}) as a function of strain, plotted as its reduced form – $G^*_{ap}/G^*_{0\,ap}$, for LBG/SiO_2 dispersions at different pH and for different particle loadings. Results obtained at higher ionic strength are also shown in Fig. 2B.

It is observed an elastic response until a certain critical strain amplitude value, after which the normalized (non-linear) modulus decreases, slightly at first and then markedly. In certain cases an extensive disruption of the system structure occurs, as it is evident by the marked decrease in the modulus. The limit of the linearity decreases with the concentration of particles. The addition of electrolyte (especially at pH 5) or lowering the pH resulted in a decrease in the value of the critical strain. Under higher ionic strength the pH effect is clearly masked (Fig. 2B). In general, the deviation from linear behaviour for the composite materials occurs at very low strains, in certain cases very close to the resolution limit of the rheometer, especially for the systems with 20 wt.% silica particles and under conditions of low ionization of the silica particles or at high ionic strength where the counter-ions can shield the charges on the silica particles. The low value of the limit of the linear viscoelastic domain clearly suggests the presence of a relatively fragile ordered structure.

A non-linear response, even at very small applied strains, is observed for diverse complex systems including waxy-oil gels (Lopes da Silva & Coutinho, 2004), protein particulate gels (Smyth, Kudryashov, & Buckin, 2001), emulsions (Bower, Gallegos, Mackley, & Madiedo, 1999), a variety of colloidal suspensions (Kinloch, Roberts, & Windle, 2002; Yziquel, Carreau, & Tanguy, 1999) and inorganic-polymer suspensions (Krishnamoorti & Yurekli, 2001; Paquien et al., 2005), and several other colloidal systems. This behaviour is usually attributable to the strain-induced disruption of the fragile structural interactions among the network forming units (low energy interactions between structural units building up the colloidal system). Similar causes should apply for our systems, as it will be discussed in the next sections.

3.3. Viscoelastic behaviour – changes with oscillatory frequency

After the time sweep tests described before, frequency sweep tests were performed to characterize the viscoelastic behaviour of the silica/polysaccharide systems. Fig. 3 shows the mechan-

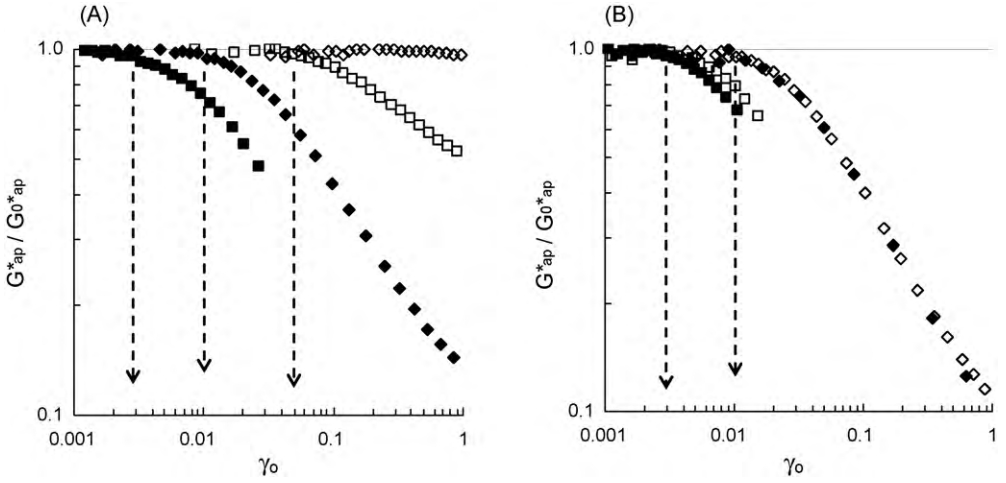

Fig. 2. The reduced complex modulus ($G^*_{ap}/G^*_{0\,ap}$) as a function of strain (γ_o) (frequency 1 rad/s and at 20 °C) for: (A) LBG/10% SiO_2 in water, at pH 3 (♦) and pH 5 (◊), and LBG/20% SiO_2 in water, at pH 3 (■) and pH 5 (□); and (B) same dispersions in 0.1 mol/dm^3 aqueous NaCl. G^*_0 denotes for the G^* at the beginning of the stress sweep experiment, after meaningful results were obtained; the dashed lines are shown as guides to the eyes for the approximate strain limits of linearity (γ_{oc}).

ical spectra (storage modulus G' and the loss modulus G'', the real and imaginary components of the complex dynamic modulus, respectively, as dependent on frequency ω) obtained for LBG/SiO_2 composite systems in water at pH 3 (Fig. 3A) and pH 5 (Fig. 3B), for different silica amounts. At low frequencies the LBG chains exhibit typical terminal behaviour with the scaling properties of approximately $G'(\omega) \sim \omega^2$ and $G''(\omega) \sim \omega$, the characteristic behaviour observed for a disordered random-coil polysaccharide in aqueous solution, where the interactions between the polymer chains are physical and temporary.

However, as the silica loading increases, this terminal behaviour disappears, and the dependence of G' and G'' on ω clearly decreases, especially at low frequencies and under conditions of low ionic charge of the particles (pH 3 or higher ionic strength). Both moduli increase but the corresponding increase in the loss modulus G'' is lower (i.e., more pronounced solid-like character of the matrix). At low frequencies, and especially at low pH, $G'(\omega)$ becomes almost independent of the frequency as particle loading increases, suggesting an onset of solid-like behaviour in these composite systems, reaching the viscoelastic behaviour typical of a solid-like (soft) material. The effect of the filler is much higher at low frequencies than at high frequencies. Nevertheless, even at high frequencies, particularly at pH 3 or at high ionic strength, one can still observe the general increase of both moduli as the silica concentration increases, i.e., the short-range dynamics of the LBG chains is also influenced by the presence of the filler particles. In water at pH 5 the slopes at high frequencies do not change much (0.92–0.73), indicating that the viscous losses at high frequency are essentially the same as for the neat polysaccharide.

The viscoelastic profile shown for the 5 wt.% SiO_2/LBG composite at pH 3 in Fig. 3A corresponds closely to the critical gel behaviour at the sol–gel threshold, characterized by a similar power-law relationship between each modulus and frequency, $G' = G''/\tan(n\pi/2) \propto \omega^n$, with $n = 0.78$. Subsequently, at some critical loading level, a crossover of the G' and G'' curves may be observed with the appearance of a plateau at low frequency and G' becomes higher than G'', what is characteristic of a liquid–gel transition as mentioned before.

At pH 5 (Fig. 3B), the sol-to-gel transition occurs for a higher amount of silica. The low-frequency power-law dependence of G' decreases monotonically with increasing particle loading, at pH 3 from $\omega^{1.7}$ to $\omega^{0.18}$ and at pH 5 from $\omega^{1.8}$ to $\omega^{0.25}$, for 0 and 20 wt.% SiO_2, respectively.

In water, at low ionic strength, clearly the higher effect of the silica particles on the rheological behaviour of the LBG solutions is observed at low pH (Fig. 3A), under conditions of low

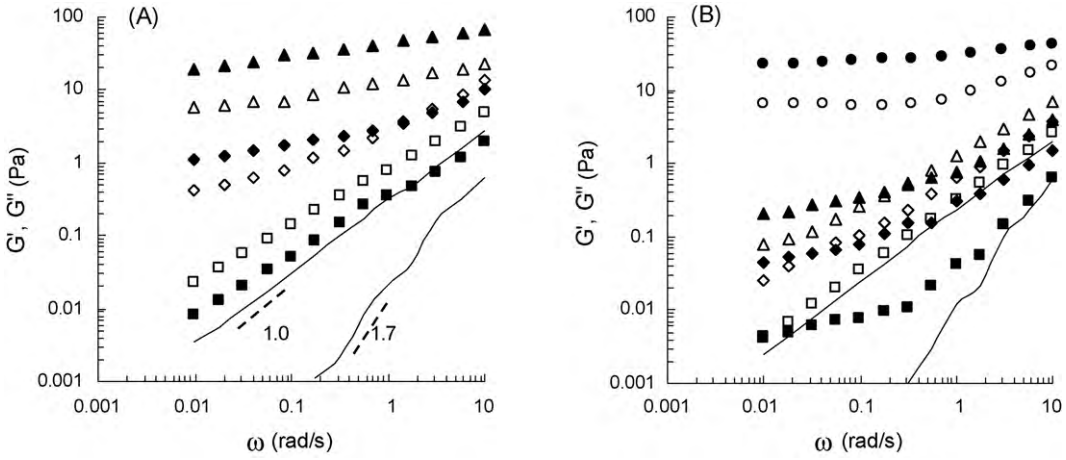

Fig. 3. Dependency of the shear viscoelastic moduli (G', solid symbols, and G'', open symbols) against the oscillation frequency (ω) for 0.5 wt.% LBG solutions, with different amounts of added silica particles, at (A) pH 3 and (B) pH 5. Lines denote for the 0.5 wt.% LBG solution, and symbols denote for the composite systems: (■, □) 5 wt.%, (♦, ◊) 10 wt.% and (▲, △) 20 wt.% silica. The mechanical spectrum for LBG/20 wt.% SiO_2 in 0.1 mol/dm^3 NaCl at pH 5 (●, ○) is also shown in (B).

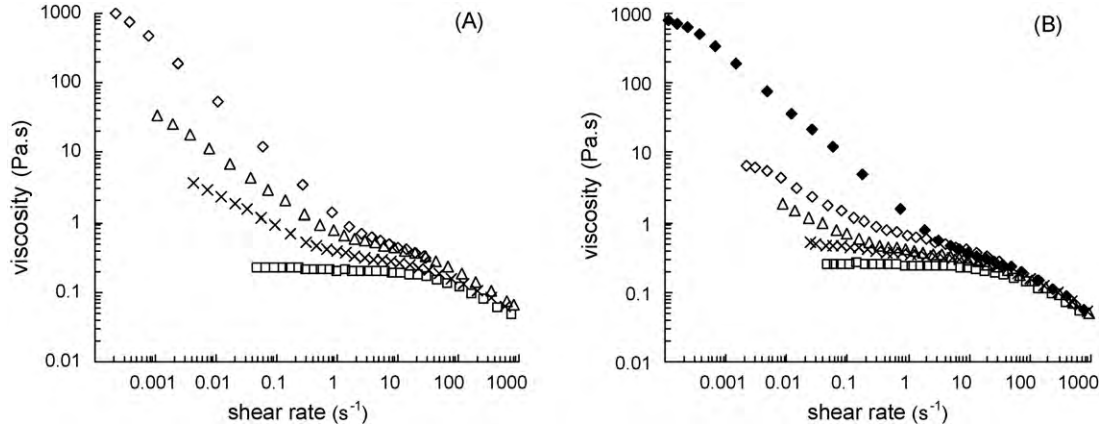

Fig. 4. Apparent viscosity as a function of shear rate at 20 °C for 0.5% LBG and LBG/SiO_2 dispersions, at (A) pH 3 and (B) pH 5: (□) neat LBG; (x) LBG + 5 wt.% SiO_2; (△) LBG + 10 wt.% SiO_2; (◊) LBG + 20 wt.% SiO_2. Also shown in (B) is the flow curve (♦) obtained for LBG + 20 wt.% SiO_2 in 0.1 mol/dm^3 NaCl at pH 5.

ionization of the silica particles. At this pH increasing the ionic strength (0.1 mol/dm^3 NaCl) only increases slightly the moduli and decreases their dependence on frequency (results not shown). However, at higher particle ionization (pH 5), increasing the ionic strength has a drastic effect on the viscoelastic behaviour; in 0.1 mol/dm^3 NaCl at pH 5 the moduli became similar to that observed at pH 3, as exemplified in Fig. 3B for the LBG/20 wt.% SiO_2 composite system.

3.4. Shear flow tests

The response of the silica/biopolymer systems to the steady-shear tests, besides given some information about the microstructure of the material and how it responds to the applied high deformations, it will also provide useful information on the material processability.

Fig. 4A shows the apparent viscosity as a function of shear rate for the 0.5% LBG solution and for the composite systems prepared at the same polysaccharide concentration and different silica loadings, at pH 3. Fig. 4B reproduces the behaviour of the composites prepared at the same biopolymer and silica concentrations but at pH 5. A flow curve obtained for LBG/20 wt.% silica at pH 5 with 0.1 mol/dm^3 NaCl is also shown in Fig. 4B to illustrate the significant effect of the salt at this pH. At pH 3 the LBG/SiO_2 composites show similar flow behaviour with or without salt addition.

The shear rate dependence of the steady-shear viscosity clearly suggests that flow modifies the composite structure, as could be expected from the high strain sensitivity already observed.

LBG exhibited the characteristic behaviour of a random-coil polysaccharide with the presence of a Newtonian viscosity plateau (η_0) at low shear rates and then a smooth transition to a power-law behaviour (shear-thinning).

The effect of the filler is observed mainly at low shear rates, namely in the shear rate range corresponding to the Newtonian plateau observed for the biopolymer solution (<10 s^{-1}). In this shear rate range, the apparent viscosity increases and diverges as the silica loading increases, the Newtonian plateau vanishes, and the composites show apparent "yield" behaviour. Qualitatively similar behaviour has been described for diverse colloidal dispersions (Kinloch et al., 2002) and many other filler/polymer nanocomposites (e.g., Paquien et al., 2005; Ren & Krishnamoorti, 2003; Solomon et al., 2001). At higher shear rates the flow behaviour of the filled systems is quite similar to that showed by the unfilled biopolymer, irrespective of filler amount, pH or ionic strength. These observations are consistent with the formation of a particle-mediated transient network, which is disrupted under shear, revealing essentially the polymer dynamics at high shear rate.

Even taking into account all the various limitations and stipulations inherent to the yield stress concept (Barnes, 1999), the yield stress is still a useful engineering parameter and has an inherent important physical meaning. In fact, the existence of yield stress has been recognized for long as a typical feature of rheological properties of filled polymers (Malkin, 1990). For the LBG/SiO_2 composites with high filler loading the apparent yielding after a critical stress has been reached is evident in the plots of viscosity as a function of shear stress (Fig. 5). The polysaccharide solution showed no yield behaviour, but this behaviour starts to change as the SiO_2 concentration increases. The typical yielding behaviour (Barnes, 1999) can be clearly observed for the composite system LBG + 20 wt.% SiO_2, with a high Newtonian viscosity at low stresses, following by a sharp drop in viscosity, about 3 orders of magnitude, over a narrow range of higher stresses, i.e., an apparent yielding at about 1 Pa.

We did not follow a semi-analytical procedure to quantify the yield stress, using one of the possible equations predicting flow with a yield stress term, e.g., Casson or Herschel–Bulkley models. Yet, based on the results obtained the LBG/silica composite suspensions show increasing apparent yield stresses as the silica loading increases, especially at pH 3 or in the presence of 0.1 M NaCl, i.e., under conditions of low charge density on filler surface.

Also shown in Fig. 5 are the upward and downward curves obtained by increasing and then decreasing the applied stresses. For the LBG solutions the up and down curves overlapped. However,

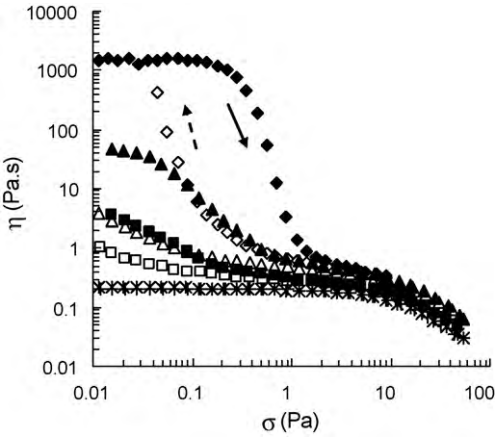

Fig. 5. Apparent viscosity (η_{ap}) as a function of shear stress (σ) at 20 °C for 0.5% LBG and LBG/SiO_2 dispersions, at pH 3, showing the upward and downward curves, resulting from first increasing the applied stress, followed by the unload of the sample at a decreasing shear stress: (× up, + down) neat LBG; (■ up, □ down) LBG + 5 wt.% SiO_2; (▲ up, △ down) LBG + 10 wt.% SiO_2; (♦ up, ◊ down) LBG + 20 wt.% SiO_2.

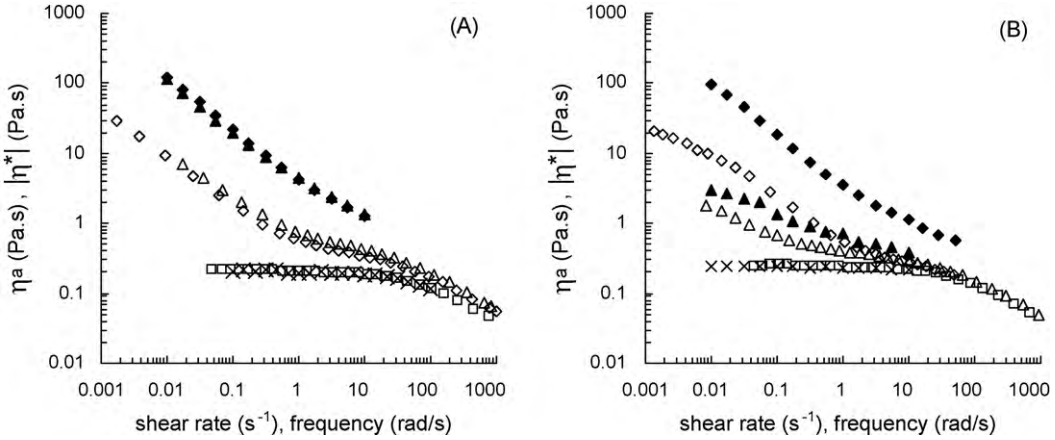

Fig. 6. Comparison of the steady-shear apparent viscosity (η_a) and the complex viscosity ($|\eta^*|$) for 0.5 wt.% LBG/10 wt.% SiO_2 samples, at 20 °C, at (A) pH 3 and (B) pH 5: (□ – η_a, x – $|\eta^*|$) neat LBG; (△ – η_a, ▲ – $|\eta^*|$) LBG + 10 wt.% SiO_2 in water; (◇ – η_a, ♦ – $|\eta^*|$) LBG + 10 wt.% SiO_2 in 0.1 mol/dm^3 NaCl.

for the LBG/silica dispersions, the up and down curves overlapped only at high stresses, but at low shear stresses, the down curve did not match the up curve anymore, the divergence being more pronounced as the silica concentration increases, suggesting a thixotropic behaviour, probably due to a partial breakdown of the weak network formed upon application of shear. The pronounced hysteresis observed for the LBG/20% SiO_2 is typical of a gel-structured material.

A thixotropic behaviour means that the viscosity of the dispersion will decrease under shear, but will return to its initial value after a rest time. However, in certain cases, if thixotropic by nature, full reversibility was not observed within the time range analysed. Also, in some cases, especially at the lower shear rates, the time to attain the stationary flow was higher than 60 s at the applied shear stress. Therefore, all time-dependent phenomena should be analysed with caution. The flow curves and the measured yield stresses can actually be transient measurements dependent on the observation time.

3.5. Cox–Merz rule

We have also compared the steady-state apparent viscosity (η_a) with the complex viscosity ($|\eta^*|$) obtained from the oscillatory experiments at low strain amplitude, in order to check the applicability of the Cox–Merz rule to our systems. The Cox–Merz rule is an empirical observation which states that the steady-shear rate viscosity and the complex viscosity are closely super-imposable for numerically equivalent values of shear rate ($\dot{\gamma}$) and frequency (ω) (Cox & Merz, 1958):

$$\eta_a(\dot{\gamma}) = \eta*(\omega) \text{ for } \dot{\gamma} = \omega$$

$$\text{with } \eta*(\omega) = \frac{G*(\omega)}{\omega} = \frac{[G'^2 + G''^2]^{1/2}}{\omega}$$

Illustrative plots are shown in Fig. 6 for the LBG/10% SiO_2 dispersions as examples of the observed behaviour. All the LBG/silica composite dispersions studied here fail to obey the Cox–Merz rule with $\eta_a(\dot{\gamma})$ always less than $\eta^*(\omega)$, being the discrepancies higher at low shear rates and for higher silica loadings. The structure of the materials is not affected under the linear oscillatory rheological tests where the strain was kept as low as possible to avoid any changes in the mesoscale structure, but the steady-shear viscosity is considerably lower than the oscillatory complex viscosity presumably because of an alteration in the mesoscale structure caused by the large displacements imposed during the steady-shear experiments.

In Fig. 6A one can observe that similar results and discrepancies to the Cox–Merz rule are observed for the LBG/silica dispersions in water or in 0.1 mol/dm^3 NaCl at pH 3. However, confirming what has been discussed above, at pH 5, for higher silica ionization (Fig. 6B) the effect of salt is clearly significant, increasing the viscosities, and more important, increasing the departure to the Cox–Merz rule. Thus the application of continuous steady-shear results in significant changes in the dissipation mechanism as compared to the quiescent or near-quiescent state structure that is dominated by the network of biopolymer chains caged on silica particle clusters.

Failures of the Cox–Merz rule have been observed for other filled polymer systems and mesostructured materials (Chatterjee & Krishnamoorti, 2008; Larson, 1999), biopolymer dispersions with either hyperentanglements or aggregates (Lopes da Silva, Rao, & Fu, 1998, Ch. 5) and complex food systems (Bistany & Kokini, 1983), and are generally associated to preferential orientation of the fillers, structure breakdown and/or disaggregation processes under the higher strains during the shear flow tests, what supports the existence of fragile networks in the biopolymer/silica dispersions under analysis.

3.6. SiO_2/LBG gel microstructure

Cryo-scanning electron microscopy was used to characterize the structure and morphology of the composite systems. Fig. 7 shows cryo-SEM images (fracture surfaces broken in liquid nitrogen) reporting the microstructure of the SiO_2/LBG systems after curing for 24 h, for different conditions.

The biopolymer chains seem to adopt stretched configurations and form a physical three-dimensional arrangement as seen by the thin fibrils or lamellar structures forming a regular meshed network. The particle distribution is not homogeneous in space. The filler silica particles are highly organized forming aggregates around the polymer fibrils. The particle clusters seem to build a case around the polymer fibrils and the polymer appears to connect the filler clusters. Increasing the amount of silica added to the polymer matrix increases the number of silica clusters, and then also the number of polymer segments that are affected by the particles, but not their average size. Changing the ionic charge of the particles, by increasing the pH (Fig. 7C) or the ionic strength (Fig. 7D) has a clear effect on the size and morphology of the particle clusters surrounding the polymer chains. The polymer network reinforced by the particle clustering and some specific biopolymer–particle and particle–particle interactions would be the main responsible for the rheological behaviour previously described.

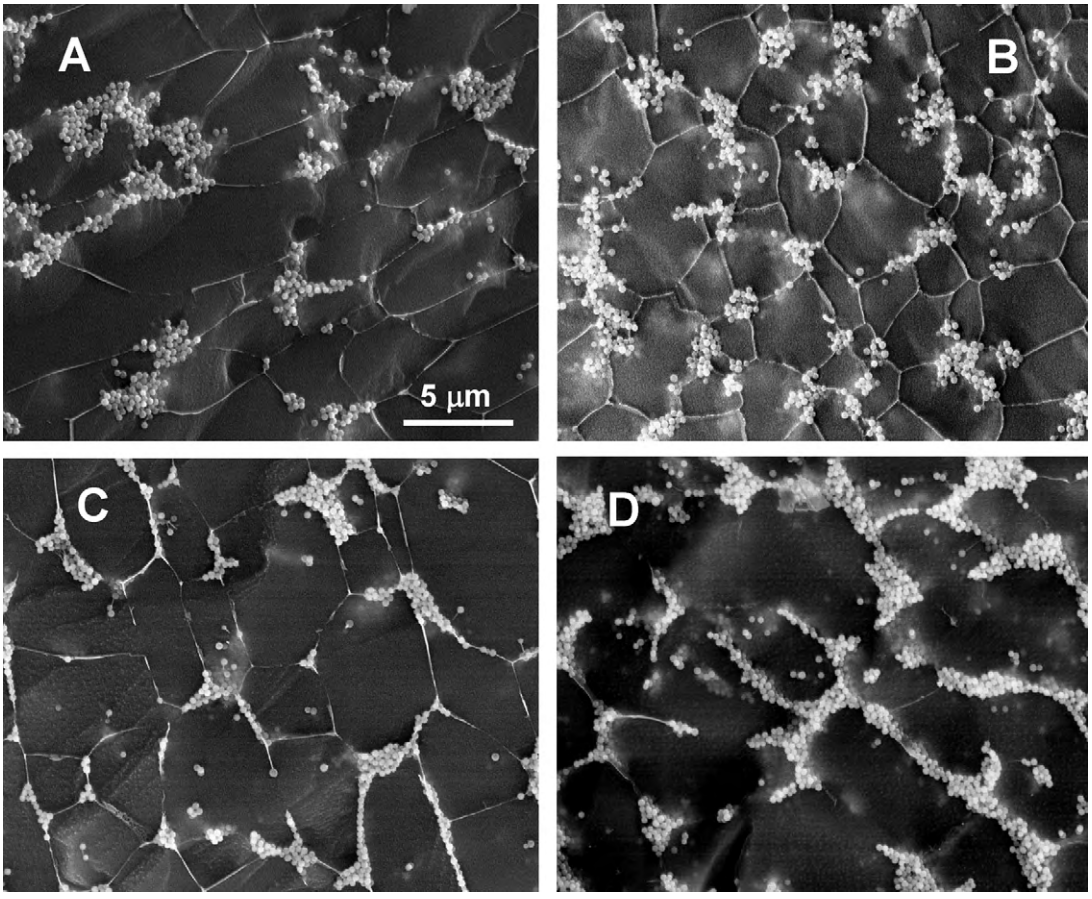

Fig. 7. Cryo-SEM images of the LBG/SiO_2 composites: (A) 10 wt.% SiO_2 in water at pH 3; (B) 20 wt.% SiO_2 in water at pH 3; (C) 10 wt.% SiO_2 in water at pH 5; (D) 10 wt.% SiO_2 in 0.1 mol/dm^3 NaCl at pH 5. One can observe that the filler particles are highly organized forming aggregates around the biopolymer fibrils. Increasing the pH (C) or the ionic strength (D) had a clear effect on the size and morphology of the particle clusters surrounding the polymer chains.

4. Discussion

Previous works on adsorption of neutral hydrophilic polymers on silica showed that neutral polymers adsorb on hydrated silica surface through hydrogen bonds (Persello, Boisvert, Guyard, & Cabane, 2004). Galactomannan adsorption on solid surfaces, namely on talc particles, has been also shown to occur mainly through hydrogen bonding (Wang & Somasundaran, 2007). Therefore, especially under conditions of low ionic density on the silica particle surface, the affinity between the galactomannan chains and silica particles is expected to be high and adsorption is expected to occur through hydrogen bonding between the polysaccharide hydroxyls and the silanol groups on the silica surface.

The microstructural analysis revealed that clusters of silica particles are not randomly dispersed within the polymer matrix. Instead, the silica particles form clusters that self-organize on the polymer fibrils or lamellar structures. However, at least for the quantities of silica analysed, there is not a continuous three-dimensional network formed by the silica particles in the entire volume of the system. Similar microstructural organization was also observed for hydrogels formed by sodium hyaluronate or cationic hydroxyethylcellulose and silica generated *in situ* by sol–gel processing (Shchipunov et al., 2005). Hence, one may envisage that the polymer chains may act as a template for silica clustering and ordering in a similar way as occurs in biomineralization processes or in the formation of silica particles by sol–gel processes in the presence of hydrophilic polymers.

This structural organization of the composite systems had significant effects upon the biopolymer rheology. Several indicators support that the composite systems exhibit weak-gel structure, being the solid-like behaviour more pronounced as the amount of the filler increases or under conditions of low ionic density of the silica particles (lower pH or higher ionic strength), i.e., those conditions that favor particle aggregation and particle–polymer interactions. The composite LBG/SiO_2 systems are characterized by long relaxation times, apparent yield stresses, and elastic moduli that are weakly dependent on strain frequency.

Particle–particle interactions building up the particle clusters and particle–polymer interactions responsible for the self-organization of the clusters around polymer domains give rise to quiescent structural evolution. In general, the LBG/SiO_2 composites show a very low linearity limit γ_o. This behaviour is attributable to the high strain sensitivity of the developed three-dimensional temporary network structures. The storage modulus of the composite materials was significantly enhanced relative to the matrix polymer, especially at pH 3, and decreased its dependence upon frequency as the silica loading increased. The modulus plateau at low frequencies is indicative of solid-like behaviour and the existence of a yield stress or at least, the existence of a specific relaxation mechanism, which appears due to the presence of the filler in the biopolymer matrix. Similar elasticity enhancement and non-terminal low frequency viscoelastic behaviour has been observed in polymer nanocomposites, mainly for filled polymer melts containing clays, carbon nanotubes, silicates, and other types of fillers (Du et al., 2004; Hyun, Lim, Choi, & Jhon, 2001; Lim, Lee, Choi, & Jhon, 2003; Potschke, Fornes, & Paul, 2002; Solomon et al., 2001) and was attributed to the formation of a filler network, which restrains the long-range motion of polymer chains. However, as discussed above,

in our case a three-dimensional network of silica particles spanning the whole sample does not appear to exist, but the continuous network seems to be guaranteed by the polymer chains.

We hypothesize that the adsorption of the silica particles along the polymer chains and the particle–particle interactions thereafter lead to weak slowing down of segmental dynamics at the polymer–solid interface and additional and/or more permanent junction zones yielding gels with enhanced elasticity. This is due to trapping of polymer chains at the filler surface which may result in a higher entanglement density. Hence, some of the biopolymer segments originally participating in simple topological entanglements (typically observed in this polysaccharide solutions) can now became elastically effective chains forming transient networks where the polymer matrix chains have much lower mobility and the rigidity of the polymer segments, between physical junction points, is reinforced by the cage of interacting particles. In addition, the presence of rigid inclusions (particle clusters) may also distort the strain field around the particles, leading to a frequency- and loading-dependent enhancement in the modulus. Interactions between particles and particle-biopolymer are labile, and although they result in a partial immobilization of the matrix chains, these labile bonds are easily ruptured under shear.

5. Conclusions

We have shown that galactomann/silica composite systems show a solid-like rheological response, with a strong dependence on silica content and ionic conditions. The microstructural analysis and the linear and non-linear rheological measurements are consistent with the composite structure of a network of particle clusters surrounding and encaging polymer fibrils and lamellar structures that exhibit several rheological properties characteristic of weak-gel systems. Somewhat surprising is the qualitative similarity observed between our systems and such diverse systems ranging from solid carbon nanotube/polycarbonate composites (Potschke et al., 2002), polymer/layered-silicate (Krishnamoorti & Yurekli, 2001) or polymer grafted to silica hybrid melts (Goel et al., 2006), to hybrid systems obtained from cationic hydroxyethylcellulose and silica generated *in situ* by sol–gel processes (Shchipunov et al., 2005) in aqueous dispersions.

An interconnected structure of silica particles was not demonstrated by direct microscopic observations. The more likely underlying mechanism for reinforcement and non-linear behaviour appears to be the confinement of polymer chains caused by the silica particle clusters. The polymer mobility is compromised by polymer imprisonment within the particle clusters and/or hindered due to adsorption at the particle surfaces. Relaxation of polymer chains is then expected to be restrained. Changes in polymer dynamics caused by the particles explain the formation of transient networks.

Appropriate manipulation of filler concentration and/or ionization yielded solid-like structured systems with complex viscoelastic behaviour, solid-like materials under quiescent conditions but flowing easily under applied stress conditions, when compared with the typical liquid-like and shear-thinning behaviour of the net polysaccharide solution. Though fragile by nature due to the marginal stability of the forces building up the network within the material, they may be tailored and lead to novel mechanical responses that may be relevant in certain application areas.

Acknowledgments

F.C. Oliveira thanks the Portuguese Foundation for Science and Technology (FCT) for a PhD grant (SFRH/BD/23396/2005).

References

Barnes, H. A. (1999). The yield stress – a review or $\pi\alpha\nu\tau\alpha$, $\rho\varepsilon\iota$ – everything flows? *Journal of Non-Newtonian Fluid Mechanics*, *81*, 133–178.
Bistany, K. L., & Kokini, J. L. (1983). Dynamic viscoelastic properties of foods in texture control. *Journal of Rheology*, *27*, 605–620.
Bower, C., Gallegos, C., Mackley, M. R., & Madiedo, J. M. (1999). The rheological and microstructural characterisation of the non-linear flow behaviour of concentrated oil-in-water emulsions. *Rheologica Acta*, *38*, 145–159.
Chatterjee, T., & Krishnamoorti, R. (2008). Steady shear response of carbon nanotube networks dispersed in poly(ethylene oxide). *Macromolecules*, *41*, 5333–5338.
Coradin, T., Allouche, J., Boissiere, M., & Livage, J. (2006). Sol–gel biopolymer/silica nanocomposites in biotechnology. *Current Nanoscience*, *2*, 219–230.
Coradin, T., Bah, S., & Livage, J. (2004). Gelatine/silicate interactions: From nanoparticles to composite gels. *Colloids and Surfaces B: Biointerfaces*, *35*, 53–58.
Cox, W. P., & Merz, E. H. (1958). Correlation of dynamic and steady flow viscosities. *Journal of Polymer Science*, *28*, 619–622.
Daniel-da-Silva, A. L., Pinto, F., Lopes-da-Silva, J. A., Trindade, T., Goodfellow, B. J., & Gil, A. M. (2008). Rheological behaviour of thermoreversible κ-carrageenan/nanosilica gels. *Journal of Colloid and Interface Science*, *320*, 575–581.
Du, F., Scogna, R. C., Zhou, W., Brand, S., Fischer, J. E., & Winey, K. I. (2004). Nanotube networks in polymer nanocomposites: Rheology and electrical conductivity. *Macromolecules*, *37*, 9048–9055.
Goel, V., Chatterjee, T., Bombalski, L., Yurekli, K., Matyjaszewski, K., & Krishnamoorti, R. (2006). Viscoelastic properties of silica-grafted poly(styrene–acrylonitrile) nanocomposites. *Journal of Polymer Science: Part B: Polymer Physics*, *44*, 2014–2023.
Hyun, Y. H., Lim, S. T., Choi, H., & Jhon, M. S. (2001). Rheology of poly(ethylene oxide)/organoclay nanocomposites. *Macromolecules*, *34*, 8084–8093.
Kinloch, I. A., Roberts, S. A., & Windle, A. H. (2002). A rheological study of concentrated aqueous nanotube dispersions. *Polymer*, *43*, 7483–7491.
Krishnamoorti, R., & Yurekli, K. (2001). Rheology of polymer layered silicate nanocomposites. *Current Opinion in Colloid & Interface Science*, *6*, 464–470.
Larson, R. (1999). *The structure and rheology of complex fluids*. New York: Oxford University Press.
Lim, S. T., Lee, C. H., Choi, H. J., & Jhon, M. S. (2003). Solidlike transition of melt-intercalated biodegradable polymer/clay nanocomposites. *Journal of Polymer Science: Part B: Polymer Physics*, *41*, 2052–2061.
Lopes da Silva, J. A., & Coutinho, J. A. P. (2004). Dynamic rheological analysis of the gelation behaviour of waxy crude oils. *Rheologica Acta*, *43*, 433–441.
Lopes da Silva, J. A., Rao, M. A., & Fu, J.-T. (1998). Rheology of structure development and loss during gelation and melting. In M. A. Rao, & R. W. Hartel (Eds.), *Phase/State Transitions in Foods* (pp. 111–157). USA: Marcel Dekker.
Malkin, A. Y. (1990). Rheology of filled polymers. *Advances in Polymer Science*, *96*, 69–97.
Metzner, A. B. (1985). Rheology of suspensions in polymeric liquids. *Journal of Rheology*, *29*, 739–775.
Oh, M. H., So, J. H., & Yang, S. M. (1999). Rheological evidence for the silica-mediated gelation of xanthan gum. *Journal of Colloid and Interface Science*, *216*, 320–328.
Paquien, J. N., Galy, J., Gerard, J. F., & Pouchelon, A. (2005). Rheological studies of fumed silica–polydimethylsiloxane suspensions. *Colloids and Surfaces A: Physicochemical and Engineering Aspects*, *260*, 165–172.
Pashkovski, E. E., Masters, J. G., & Mehreteab, A. (2003). Viscoelastic scaling of colloidal gels in polymer solutions. *Langmuir*, *19*, 3589–3595.
Persello, J., Boisvert, J. P., Guyard, A., & Cabane, B. (2004). Structure of nanometric silica clusters in polymeric composite materials. *Journal of Physical Chemistry B*, *108*, 9678–9684.
Pinto, R. J. B., Marques, P. A. A. P., Barros-Timmons, A. M., Trindade, T., & Neto, C. P. (2008). Novel SiO_2/cellulose nanocomposites obtained by *in situ* synthesis and via polyelectrolytes assembly. *Composites Science and Technology*, *68*, 1088–1093.
Potschke, P., Fornes, T. D., & Paul, D. R. (2002). Rheological behaviour of multiwalled carbon nanotube/polycarbonate composites. *Polymer*, *43*, 3247–3255.
Ren, J., & Krishnamoorti, R. (2003). Nonlinear viscoelastic properties of layered-silicate-based intercalated nanocomposites. *Macromolecules*, *36*, 4443–4451.
Shchipunov, Y. A., & Karpenko, T. Y. (2004). Hybrid polysaccharide-silica nanocomposites prepared by the sol–gel technique. *Langmuir*, *20*, 3882–3887.
Shchipunov, Y. A., Karpenko, T. Y., Krekoten, A. V., & Postnova, I. V. (2005). Gelling of otherwise nongelable polysaccharides. *Journal of Colloid and Interface Science*, *287*, 373–378.
Smyth, C., Kudryashov, E. D., & Buckin, V. (2001). High-frequency shear and volume viscoelastic moduli of casein particle gel. *Colloids and Surfaces: A: Physicochemical and Engineering Aspects*, *183–185*, 517–526.
Solomon, M. J., Almusallam, A. S., Seefeldt, K. F., Somwangthanaroj, A., & Varadan, P. (2001). Rheology of polypropylene/clay hybrid materials. *Macromolecules*, *34*, 1864–1872.
Trompette, J. L., & Bordes, C. (2000). Rheological study of the gelation kinetics of a concentrated latex suspension in the presence of nonadsorbing polymer chains. *Langmuir*, *16*, 9627–9633.
Trompette, J. L., Charnay, C., & Partyka, S. (1998). Storage stability and rheological behaviour of talc-polyacrylylglycinamide gelified suspensions. *Langmuir*, *14*, 4475–4481.

Wang, J., & Somasundaran, P. (2007). Study of galactomannan interaction with solids using AFM, IR and allied techniques. *Journal of Colloid and Interface Science*, *309*, 373–383.
Yziquel, F., Carreau, P. J., & Tanguy, P. A. (1999). Non-linear viscoelastic behaviour of fumed silica suspensions. *Rheologica Acta*, *38*, 14–25.
Zhang, Q., & Archer, L. A. (2002). Poly(ethylene oxide)/silica nanocomposites: Structure and rheology. *Langmuir*, *18*, 10435–10442.
Zou, H., Wu, S., & Shen, P. (2008). Polymer/silica nanocomposites: Preparation, characterization, properties, and applications. *Chemical Reviews*, *108*, 3893–3957.